CHAPTER 12: COORDINATION CHEMISTRY IV: REACTIONS AND MECHANISMS

12.1 $[Cr(H_2O)_6]^{2+}$ is labile, and has 4 unpaired electrons, with 1 in the anti-bonding e_g orbital. Occupation of this orbital renders substitution easier by leading to relatively weak chromium(II)–aqua ligand bonds. $[Cr(CN)_6]^{4-}$ is inert. It has all 4 metal valence electrons in the bonding t_{2g} levels. These orbitals are rendered bonding in character due to π-backbonding with the cyanide ligands.

12.2 If the rate constants for different entering ligands are significantly different, it suggests that increasing the coordination number is important in the rate-determining step. A necessary assumption to make this assertion is that the mechanism via which the complex undergoes substitution does not vary with the entering ligand.

12.3 Pentachlorooxochromate(V) is a d^1 complex; it should be labile, with vacancies in the t_{2g} levels.

Hexaiodomanganate(IV) is a d^3 complex; it should be inert.

Hexacyanoferrate(III) is a low-spin d^5 complex; it should be inert (vacant e_g levels).

Hexammineiron(III) is a d^6 high-spin complex; with partly occupied orbitals in both levels; it should be labile.

12.4 The $[Fe(CN)_6]^{4-}$ ion is a low-spin d^6 complex, with a maximum LFSE of $-2.4\ \Delta_o$. It is a notably kinetically inert complex, hence its low reactivity towards ligand substitution that would release the potentially toxic cyanide.

12.5 $[Fe(H_2O)_6]^{3+}$ and $[Co(H_2O)_6]^{2+}$ are high-spin species; the electrons in the upper e_g levels render them labile. $[Cr(CN)_6]^{4-}$ is a d^4 low-spin species. The t_{2g} levels are unequally occupied and the e_g are vacant, which makes it a borderline complex in terms of substitution rate. $[Cr(CN)_6]^{3-}$, $[Fe(CN)_6]^{4-}$, and $[Co(NH_3)_5(H_2O)]^{3+}$ are low-spin species with the t_{2g} levels either half filled or completely filled. This, combined with empty e_g levels, indicates inert species. LFAE approximations suggest that the activation energies for substitution reactions with these ions are relatively large.

12.6 The general rate law for square planar substitution is: Rate = $(k_1 + k_2[Cl^-])\ [[Pt(NH_3)_4]^{2+}]$.

The general procedure is to measure either the disappearance of $[Pt(NH_3)_4]^{2+}$ or the formation of $[Pt(NH_3)_3Cl]^+$ to find the reaction rate. The most convenient method is by UV or visible absorbance spectra, using a wavelength where there is a large difference in absorbance between the two species. One experimental strategy would be to attempt to establish pseudo-first order conditions, by using a significantly large chloride concentration, so that its concentration can be assumed to not change appreciably while the reaction rate is measured. This may make the reaction appear first order in Pt reactant. Measure the change in reactant and product concentrations using spectroscopy. A plot $\ln([Pt(NH_3)_4^{2+}])$ versus time will afford a straight line with slope k_{obs} if the pseudo-first order approximation is valid when excess chloride is used. Assuming this approximation holds, repeat several times with different (but all sufficiently high) chloride concentrations. A graph k_{obs} vs. $[Cl^-]$ will result in a straight line with intercept = k_1 and slope = k_2.

12.7 **a.** DMSO exchange is extremely fast since this is present in large excess as the solvent.

b. Saturation kinetics occurs with these entering ligands, as increasing $[X^-]$ results in apparent plateaus of the rate constant. The largest of these rate constants (for nitrate) is slightly more than an order of magnitude larger than that of thiocyanate, suggesting the incoming ligand may play a significant role in influencing the rate. The limiting rate constant at high $[X^-]$ suggests that either a D mechanism, I_d mechanism (if we assume that these substitution reactions are irreversible), or one involving a preassociation complex are viable options.

c. Application of a steady-state approximation for a possible *D* mechanism provides a rate law of $\text{Rate} = k_{obs}\left[\left[\text{Co(en)}_2(\text{NO}_2)(\text{DMSO})\right]^{2+}\right]$ where $k_{obs} = k_1$ when the concentration of entering ligand is high. A vital issue is whether these k_1 values are sufficiently similar when the chloride, nitrate, and thiocyanate trials are compared to justify assignment of a *D* mechanism. Ideally, k_1 would be expected to be independent of the incoming ligand if a *D* mechanism were operative. For the possibility of assessing whether an I_d mechanism is operative with these data, it is necessary to assume that the substitution is irreversible. In this case, when the concentration of entering ligand is high, pseudo-first order conditions can be assumed, and the rate law simplifies to $\text{Rate} = k_{obs}\left[\left[\text{Co(en)}_2(\text{NO}_2)(\text{DMSO})\right]^{2+}\right]$ where $k_{obs} = k_1[X^-]$.

d. The similarity in the k_1 values when those of chloride, nitrate, and thiocyanate are compared for both *D* (where $k_{obs} = k_1$) and I_d possibilities (where $k_{obs} = k_1[X^-]$ assuming the substitution reaction is irreversible) suggests that these mechanisms are both viable possibilities. However, the variation in these rate constants with different entering ligands indicates that the entering ligand likely plays some role in the rate determining step, rendering an I_d mechanism as perhaps a better hypothesis. The possibility of a preassociation complex mechanism could also be argued, but more data is needed to properly evaluate this possibility.

12.8 **a.** Because the rate is independent of the concentration of ^{13}CO, the rate determining step is most likely:

$$Cr(^{12}CO)_6 \longrightarrow Cr(^{12}CO)_5 + {}^{12}CO$$

$Cr(^{12}CO)_5$ then reacts rapidly with ^{13}CO.

b. These terms describe two pathways to product, a dissociative pathway (as in part **a**) and an associative pathway:

Dissociative: $Cr(CO)_6 \longrightarrow Cr(CO)_5 + CO$ (slow) rate = $k_1[Cr(CO)_6]$
$Cr(CO)_5 + PR_3 \longrightarrow Cr(CO)_5(PR_3)$ (fast)

Associative: $Cr(CO)_6 + PR_3 \longrightarrow Cr(CO)_5(PR_3) + CO$ rate = $k_2[Cr(CO)_6][PR_3]$

With two mechanistic pathways leading to the same product, the overall rate is the sum of the rates of both.

c. Bulky ligands will tend to favor the first order (dissociative pathway) because the crowding around the metal will favor dissociation and hinder association with incoming ligands. (This effect is discussed further in Section 14.1.1)

12.9 $[Cu(H_2O)_6]^{2+}$ is a d^9 complex, subject to Jahn-Teller distortion. Therefore, different rates are observed for exchange of axial and equatorial water molecules.

12.10 These exchange reactions are interesting since the reactants and products have the same structures and energies. The hypothesized mechanism for $[Li(H_2O)_4]^+$ water exchange is shown below.

In **A**, a water molecule in the second coordination sphere interacts weakly with the lithium center and one aqua ligand via hydrogen bonding. This solvated $[Li(H_2O)_4(H_2O)]^+$ species is more thermodynamically stable than separated $[Li(H_2O)_4]^+$ and H_2O. In the transition state **B**, the incoming water molecule approaches the metal center and pushes two aqua ligands towards the axial positions of the approximately trigonal bipyramidal intermediate **C**, with the incoming H_2O in an equatorial site. Calculations suggest that the molecular volume of intermediate **C** is less than that of **B**, supporting a limiting associative mechanism (*A*).

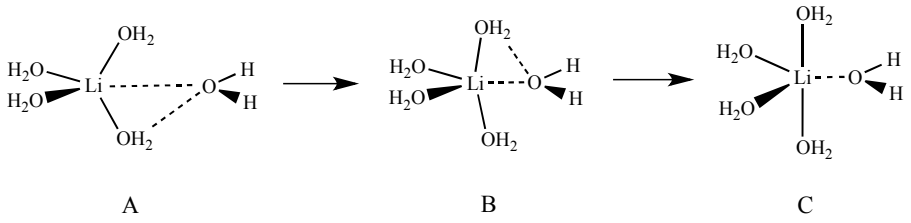

A B C

The mechanism for ammonia ligand exchange for $[Li(NH_3)_4]^+$ is proposed to follow an alternate mechanism that also begins with a solvated $[Li(NH_3)_4(NH_3)]^+$ that is more thermodynamically stable than separated $[Li(NH_3)_4]^+$ and NH_3. In the lowest energy solvated $[Li(NH_3)_4]^+$ species (**D**), the NH_3 molecule is proposed to interact simultaneously with N—H bonds of two ammine ligands. Transition state **E** is approximately trigonal bipyramidal with the entering and leaving ammine ligands positioned in axial sites. An associative interchange mechanism (I_a) is inferred on the basis of molecular volume calculations that indicate that the volume of **E** is nearly the same as that of **D** (the bonds in **E** are long).

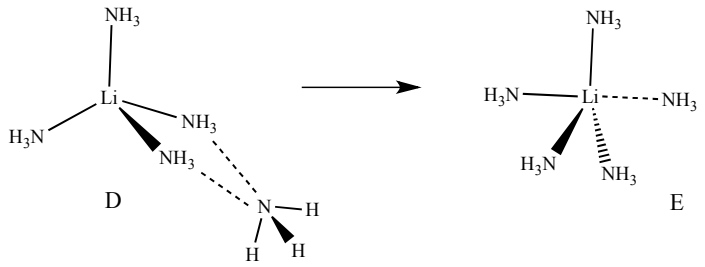

D E

12.11 A plot of k_{obs} versus $[As(C_6H_5)_3]$ exhibits a linear relationship, with intercept $k_1 = 2.3 \times 10^{-5}$ s^{-1} and slope $k_2 = 2.06 \times 10^{-5}$ $M^{-1}s^{-1}$.

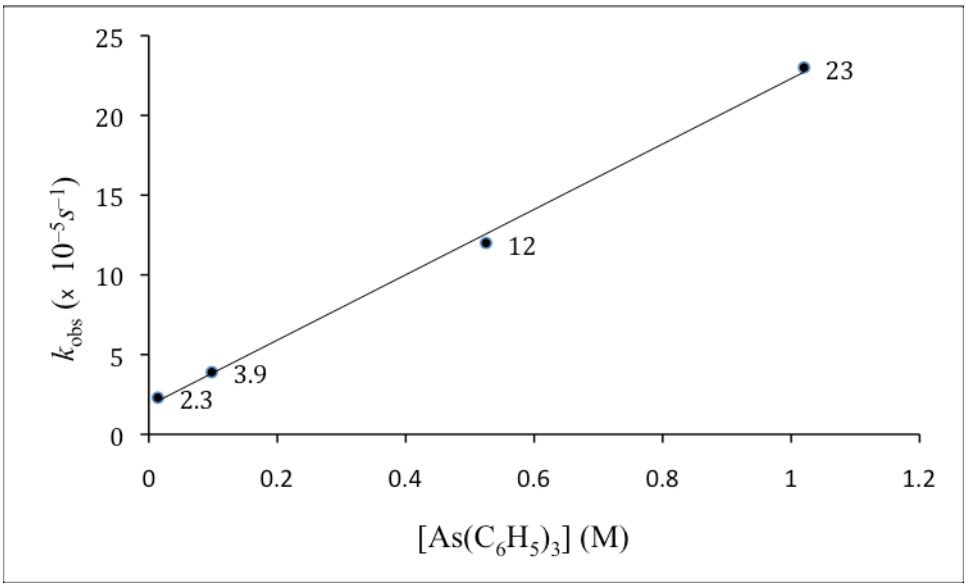

$$\text{Rate} = (k_1 + k_2[As(C_6H_5)_3])[Co(NO)(CO)_3]$$

This reaction shows both first and second order kinetics; the ligand substitution likely occurs via two mechanisms. The first order reaction appears to be a dissociative reaction or a solvent-assisted dissociation of CO, followed by a fast addition of $As(C_6H_5)_3$. The other path shows first order dependence on $As(C_6H_5)_3$, perhaps caused by an associative reaction.

12.12 ΔHNP is a measure of basicity, with more basic molecules having a smaller ΔHNP. The reactions appear to be associative, with the rate increasing with the basicity of the incoming ligand. The two lines are a consequence of the different natures of the ligands; numbers 1-11 are all phosphorus ligands, while 12-14 are organic nitrogen compounds. The half neutralization potential provides a relative measure of basicity within compounds of similar structure, but is not an absolute measure of the reactivity of the compounds.

12.13 **a.** $\Delta G° = \Delta H° - T\Delta S° = 10300 - 298 \times 55.6 = -6300$ J/mol $= -6.3$ kJ/mol

$\Delta G° = -RT \ln K$; $\ln K = -\Delta G°/RT = 6300/(8.3145 \times 298.15) = 2.54$; $K = 12.7$

b. The *cis* isomer has the higher bond energy (actually, the lower overall energy and collectively stronger bonding), since rearrangement to the *trans* isomer is endothermic. Since the phosphines are better π acceptors, the *cis* isomer should be the more stable. If the phosphines are mutually *trans*, they compete for overlap with the same *d* orbitals, resulting in weaker bonds to Pt(II). When these phosphines are mutually *cis*, each can use one of the pair of d_{xz} and d_{yz} orbitals and avoid competition.

c. The free phosphine must aid the isomerization via an associative mechanism. Since benzene is the solvent, and it is very nonpolar, it is not likely to assist the reaction. Only the second term of the rate equations of Problem 12.6 is significant here, with phosphine playing the role of the entering ligand.

12.14 Two factors need to be considered:

1. The best π acceptors (CO, PPh_3) slow the dissociation of CO in the *cis* position; π donors (halides) speed the dissociation.

2. Halides are weaker σ donors relative to phosphines and carbon monoxide. As a result, there is less electron density available for π-back-bonding in the complexes with halide ligands. This results in weaker M—CO bonds in these complexes, which lowers the activation energy for CO dissociation by raising the electronic ground state of the starting complex. The π-donor ability of these halides also assists in stabilizing the square-pyramidal transition state, further contributing to a lowering of the activation energy for CO dissociation.

12.15 *Trans*-$Pt(NH_3)_2Cl_2$ reacts with thiourea (tu) to form *trans*-$[Pt(NH_3)_2(tu)_2]^{2+}$; the first Cl^- is displaced and the strong *trans* effect of tu leads to preferential replacement of the second Cl^-.

Both chlorides of *cis*-$Pt(NH_3)_2Cl_2$ are initially replaced. The tu's are then *trans* to the NH_3's, which are replaced because of the strong *trans* effect of tu, resulting in $[Pt(tu)_4]^{2+}$.

12.16 **a.** $[Pt(CO)Cl_3]^- + NH_3 \rightarrow$ *trans*-$[Pt(CO)(NH_3)Cl_2]$ CO is the stronger *trans* director

b. $[Pt(NH_3)Br_3]^- + NH_3 \rightarrow$ *cis*-$[Pt(NH_3)_2Br_2]$ Br is the stronger *trans* director

c. $[Pt(C_2H_4)Cl_3]^- + NH_3 \rightarrow$ *trans*-$[Pt(C_2H_4)(NH_3)Cl_2]$ C_2H_4 is the stronger *trans* director.

12.17 **a.** Two sets of reactions, with examples from Figure 12.13 identified:

$[PtCl_4]^{2-} + 2NH_3 \rightarrow$ *cis*-$[PtCl_2(NH_3)_2] + 2\ Cl^-$ (b)

cis-$[PtCl_2(NH_3)_2] + 2\ py \rightarrow$ *cis*-$[Pt(py)_2(NH_3)_2]^{2+} + 2\ Cl^-$ (h)

cis-$[Pt(py)_2(NH_3)_2]^{2+} + 2\ NO_2^- \rightarrow$ *trans*-$[Pt(NO_2)_2(NH_3)(py)] + NH_3 + py$ (e)

trans-$[Pt(NO_2)_2(NH_3)(py)] + CH_3NH_2 \rightarrow$

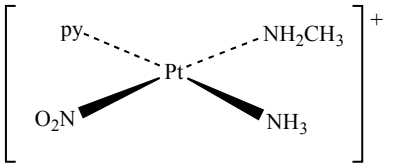

$+ \quad NO_2^-$ (g)

(Continued on next page)

$[PtCl_4]^{2-} + 2\ py \rightarrow cis\text{-}[PtCl_2(py)_2] + 2\ Cl^-$ (b)

$cis\text{-}[PtCl_2(py)_2] + 2\ CH_3NH_2 \rightarrow cis\text{-}[Pt(CH_3NH_2)_2(py)_2]^{2+} + 2\ Cl^-$ (h)

$cis\text{-}[Pt(CH_3NH_2)_2(py)_2]^{2+} + 2\ NO_2^- \rightarrow$
$trans\text{-}[Pt(NO_2)_2(CH_3NH_2)(py)] + py + CH_3NH_2$ (c)

$trans\text{-}[Pt(NO_2)_2(CH_3NH_2)(py)] + NH_3 \rightarrow$

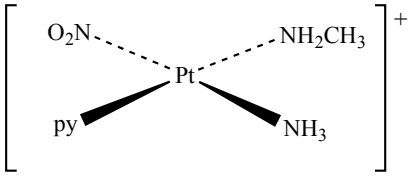

(a)

b. Reaction with Cl_2 puts Cl both above and below the plane, with the products

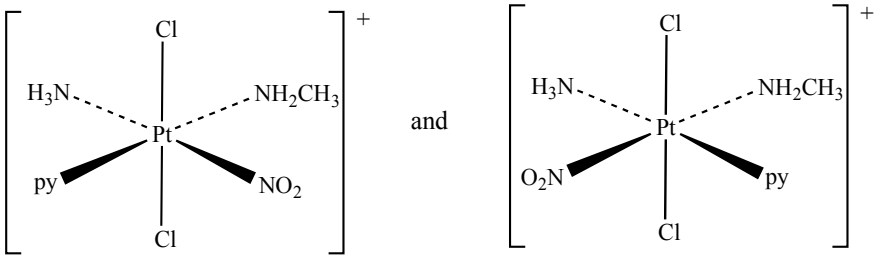

Reaction with one mole of Br^- replaces one Cl^-, with the products

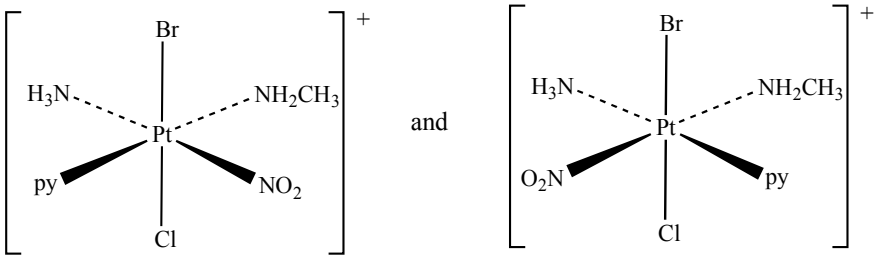

12.18 **a.** The large negative entropy of activation implies that the activated complex is much more ordered than the reactants. This suggests an associative pathway.

b. The iodo ligand leads to the fastest rate, involving bond breaking *trans* to the halogen, and therefore has the strongest *trans* effect.

12.19 V^{2+} is d^3, and likely to be inert. V^{3+} is d^2, and labile. At low $[H^+]$ (slightly basic conditions), an equilibrium mixture of $[V(H_2O)_6]^{3+}$ and $[V(H_2O)_5OH]^{2+}$ may persist. The hydroxo ligand of $[V(H_2O)_5OH]^{2+}$ may permit a bridging interaction with labile $[V(H_2O)_6]^{2+}$ to form $[V(H_2O)_5(\mu\text{-}OH)V(H_2O)_5]^{4+}$ to facilitate an inner sphere electron transfer mechanism. A proposed rate law is below, with *a* and *b* determining the relative rates of the two paths, where term *a* is associated with an outer sphere electron transfer and term *b* is associated with an inner sphere pathway. In path *a*, the bimolecular rate-determining step is the outer sphere electron

transfer while in path *b* the rate-determining step is the bimolecular formation of the bridging hydroxo complex.

$$\text{Rate} = (k_1 + k_2/[H^+])[V^{2+}][V^{3+}], \text{ so } a = k_1\,[V^{2+}][V^{3+}] \text{ and } b = k_2[V^{2+}][V^{3+}]$$

12.20 $[Cr(H_2O)_6]^{2+}$ is labile, but $[Co(NH_3)_6]^{3+}$ is inert, and the NH_3 ligands are not well equipped to bridge two metals. Therefore, the reaction is likely to be an outer-sphere reaction.

12.21 This reaction is inner sphere, so the X^- serves as a bridging ligand and a conduit for the electron transfer. The order of rates is $Br^- > Cl^- > N_3^- > F^- > NCS^-$. The difference in reaction rate is most strongly correlated to the varying abilities of these bridging ligands to accommodate electron transfer between the metal centers. Br^- works best, and this could be rationalized by estimating that the hard-soft compatibility of Cr^{2+} and Br^- is optimum among these ligands, leading to a relatively robust bridging interaction. Chloride is slightly harder, leading to a slightly lower electron transfer rate. F^- is apparently too hard; the high effective nuclear charge its valence electrons experience render it a poor conduit for electron transfer to Cr^{2+}. The NCS^- ligand offers a very slow electron transfer, the Cr—NCS—Cr bridge features one interaction with better HSAB compatibility than the other; the resulting bridge must not be ideal for electron transfer despite the presence of a conjugated π-system that can lower the activation barrier for electron transfer. Azide also has a conjugated system, but the Cr-NNN-Cr interactions apparently do not have an optimal HSAB match (nitrogen is too hard) to permit a suitable interaction. It is somewhat surprising that azide results in a faster electron transfer rate relative to thiocyanate on the basis of solely HASB arguments. The data in this problem are from D.L. Ball and E. L. King, *J. Am. Chem. Soc.*, **1958***, 80*, 1091.

12.22 **a.** NSe has the stronger *trans* effect. The longer Os—N_1 distance is consistent with weakening of this bond by the ligand *trans* to it, the NSe ligand.

b. The short bond distance and large Os—N—Se angle (164.7°) suggest that the ligand has NSe^+ character; the cation NSe^+ would have a bond order of 3 and a very short bond-bond distance. It is also worth noting that the N–Se stretching vibration in this complex is much higher (by 211 cm^{-1}) than in gas phase NSe.

12.23 **a.** The more rapid reactivity of the Mn complex is consistent with the general observation that first row transition metal complexes are generally more substitutionally labile than second and third row complexes.

b. The negative volume of activation is consistent with an *A* (or I_a) mechanism.

c. Occurrence of two infrared bands is more consistent with a *fac* isomer; a *mer* isomer is predicted by symmetry to have three IR-active bands:

<u>*mer* isomer (C_{2v}):</u>

C_{2v}	E	C_2	σ (xz)	σ (yz)	
Γ	3	1	3	1	
A_1	1	1	1	1	z
B_1	1	–1	1	–1	x

The representation Γ reduces to 2 $A_1 + B_1$, all IR-active. Three IR-active carbonyl bands are expected.

fac isomer (C_{3v}):

C_{3v}	E	2 C_3	3 σ_v	
Γ	3	0	1	
A_1	1	1	1	z
E	2	–1	0	(x, y)

The representation Γ reduces to $A_1 + E$, both IR-active. Two IR-active carbonyl bands are expected.

12.24 These data support ring-closing reactions with dissociative activation. The uniformly positive ΔS_{act} values suggest transition states in the rate determining steps where cyanide ligand dissociation is more prominent than coordination of the pyridine-carboxylate nitrogen atom to the Mn(V) center. The similarity in the rate constants (the average k_1 is $1.03 \times 10^{-3}\, M^{-1}s^{-1}$ with a standard deviation of only $1.3 \times 10^{-4}\, M^{-1}s^{-1}$) is remarkable. These rate constants appear independent of the different nitrogen atom basicities and the charges of these pyridine-carboxylates. Varying these properties of the entering ligand has very little impact on the speed of cyanide substitution. This is also consistent with dissociative activation.

12.25 **a**. The consumption rates of U^{4+} and $[PtCl_6]^{2-}$ were monitored with UV-Vis spectroscopy, by monitoring the absorptions of U^{4+} (λ_{max} = 648 nm) and $[PtCl_6]^{2-}$ (λ_{max} = 300 nm) with time. Reaction orders with respect to both of these ions were determined to be 1 on the basis of the linear relationships of the plots of $\ln(A_\infty - A_t)$ versus time, where A_∞ and A_t are the absorbances at time t and infinite time for U^{4+} and $[PtCl_6]^{2-}$, respectively. These plots exhibited linear relationships for more than three half-lives.

b. One hypothesis is that $[U(H_2O)_n]^{4+}$ initially forms a complex with $[PtCl_6]^{2-}$ that subsequently loses two protons to yield a neutral intermediate where $[PtCl_6]^{2-}$ is coordinated to $[U(H_2O)_{n-2}(OH)_2]^{2+}$ via hydroxide bridges (shown at right). The inner-sphere electron transfer of two electrons from U(IV) to Pt(IV) is proposed to proceed via this complex. The activation barrier for electron transfer via this intermediate may be reduced (leading to a faster reaction) since the U fragment closely resembles the ultimate uranium(VI)-containing product $[(H_2O)_{n-2}UO_2]^{2+}$.

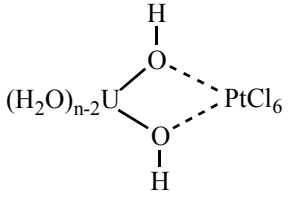

12.26 **a**. These complexes have been established as outer-sphere reactants in previous work.

b. Using the reaction of $[Co(edta)]^-$ and $[Fe(CN)_6]^{4-}$ as an example, the rate law is proposed as $\text{Rate} = k_1\left[[Fe(CN)_6]^{4-}\right]\left[[Co(edta)]^-\right]$, first order with respect to each complex. To create a graph such as that shown in Figure 3 of the reference, a series of reactions were conducted with varying, but always excess $[Fe(CN)_6]^{4-}$ and a smaller fixed concentration of $[Co(edta)]^-$. The concentration of $[Fe(CN)_6]^{4-}$ is assumed to not change significantly during these trials, allowing the rate law to be expressed as $\text{Rate} = k_{obs}\left[[Co(edta)]^-\right]$ where $k_{obs} = k_1\left[[Fe(CN)_6]^{4-}\right]$. The k_{obs} rate constants were determined and then plotted versus the $[Fe(CN)_6]^{4-}$ concentration for each trial. The linear relationship and the zero *y*-intercept support the validity of the pseudo-first order conditions, and that the overall bimolecular rate law is operative in these electron transfer reactions. The relationship between k_{obs} and k_1 is $k_{obs} = k_1\left[[Fe(CN)_6]^{4-}\right]$, and the slope of the plot of k_{obs} versus $\left[[Fe(CN)_6]^{4-}\right]$ provides the bimolecular rate constant k_1. This is a beautiful example of the application of pseudo-first order conditions.

c. The hypothesis is that the reactants become compartmentalized, hindering their ability to encounter each other for electron transfer, in the presence of reverse micelle (RM) microemulsions. $[Co(edta)]^-$ is believed to penetrate into the interfacial region of the RM, while $[Fe(CN)_6]^{4-}$ access to this region is limited, confining $[Fe(CN)_6]^{4-}$ to the aqueous solution. The physical separation of these complexes may be the dominant factor in hindering the electron transfer reaction, but the possibility that the reduction potentials of these complexes may be changed (for example, that $[Co(edta)]^-$ may be rendered a weaker oxidizing agent when embedded in the interfacial region of the RM) is also mentioned.